

Nanoscale

Accepted Manuscript



This is an *Accepted Manuscript*, which has been through the Royal Society of Chemistry peer review process and has been accepted for publication.

Accepted Manuscripts are published online shortly after acceptance, before technical editing, formatting and proof reading. Using this free service, authors can make their results available to the community, in citable form, before we publish the edited article. We will replace this *Accepted Manuscript* with the edited and formatted *Advance Article* as soon as it is available.

You can find more information about *Accepted Manuscripts* in the [Information for Authors](#).

Please note that technical editing may introduce minor changes to the text and/or graphics, which may alter content. The journal's standard [Terms & Conditions](#) and the [Ethical guidelines](#) still apply. In no event shall the Royal Society of Chemistry be held responsible for any errors or omissions in this *Accepted Manuscript* or any consequences arising from the use of any information it contains.



Received 00th January 20xx,

Stable and efficient colour enrichment powders of nonpolar nanocrystals in LiCl†

Accepted 00th January 20xx

Talha Erdem,^{a,†} Zeliha Soran-Erdem,^{a,†} Vijay Kumar Sharma,^b Yusuf Kelestemur,^a Marcus Adam,^c Nikolai Gaponik,^c and Hilmi Volkan Demir^{a,b,*}

DOI: 10.1039/x0xx00000x

www.rsc.org/

In this work, we propose and develop the inorganic salt encapsulation of semiconductor nanocrystal (NC) dispersion in nonpolar phase to make highly stable and highly efficient colour converting powder for colour enrichment in light-emitting diode backlighting. Here the wrapping of as-synthesized green-emitting CdSe/CdZnSeS/ZnS nanocrystals into a salt matrix without ligand exchange is uniquely enabled by using LiCl ionic host dissolved in tetrahydrofuran (THF), which simultaneously disperses these nonpolar nanocrystals. We studied the emission stability of the solid films prepared using NCs with and without LiCl encapsulation on blue LEDs driven at high current levels. The encapsulated NC powder in epoxy preserved 95.5% of the initial emission intensity and stabilized at this level while the emission intensity of NCs without salt encapsulation continuously decreased to its 34.7% after 96 h of operation. In addition, we investigated the effect of ionic salt encapsulation on the quantum efficiency of nonpolar NCs and found the quantum efficiency of the NCs-in-LiCl to be 75.1% while that of the NCs in dispersion was 73.0% and that in film without LiCl encapsulation was 67.9%. We believe that such ionic salt encapsulated powders of nonpolar NCs presented here will find ubiquitous use for colour enrichment in display backlighting.

1. Introduction

Within the thirty years following their first report¹, colloidal nanocrystals (NCs) have witnessed a tremendous improvement in their synthesis, crystal quality, and quantum efficiency². As a consequence of these developments, today NCs have been extensively used in various applications from biology³ to optoelectronics including light-emitting diodes (LEDs)⁴⁻⁶ and lasers^{7,8}. In particular, the tunability of the NC emission and its narrow bandwidth have attracted significant attention for their use in display backlighting⁹ and general lighting^{4,5} as colour converters on light-emitting diodes. Despite their improved quantum efficiencies, the NCs still remain vulnerable to the solid film preparation process using polymer based encapsulants since the quantum efficiencies of the NCs significantly decrease in the polymer film. In addition, due to the continuous exposure to energetic photons and elevated temperatures, the emission intensity of the NCs decreases undesirably on light-emitting diodes (LEDs). Especially, the use of these LEDs for long durations causes

significant degradation of NC emission. To improve the emission stability of the NCs, silica coating was proposed; however, this eventually adversely affects the quantum efficiency of the NCs¹⁰. As an alternative, Otto et al. demonstrated for the first time that aqueous NCs can be incorporated in a single phase process in salt crystals (e.g., NaCl, KCl, etc.) and this improves the emission stability of the NCs¹¹. Another study reported by Müller et al. showed that these salt crystals also improve the quantum efficiency of the aqueous NCs¹². Subsequently, we applied this single-phase approach to plasmonic systems and demonstrated plasmonic fluorescence enhancement of the aqueous NCs this time together with the aqueous metal nanoparticles co-immobilized in sucrose host crystals¹³. In all these previous reports,¹¹⁻¹⁴ however, only aqueous NCs (or other aqueous nanoparticles) could be used. In the case of using aqueous NCs, the as-synthesized NCs in water are plagued with intrinsically low quantum efficiencies. Alternatively, high-efficiency nonpolar NCs could be used only after ligand exchange, which also suffered from substantially reduced quantum efficiencies upon the ligand exchange. Therefore, in either case, the quantum efficiency of the resulting ionic salt encapsulated aqueous NCs in a single phase has been a problem. However, the utilization of nonpolar NCs is significantly important because of their high efficiencies and narrow emission bandwidths. Acquiring a narrow emission is very essential for the displays and general lighting applications while high quantum efficiencies in particular in the blue-green colours are needed to address the green gap problem of the epitaxial LEDs^{4,5}.

^a Departments of Electrical and Electronics Engineering, Physics, UNAM–National Nanotechnology Research Center, and Institute of Materials Science and Nanotechnology, Bilkent University, 06800, Turkey. E-mail: volkan@bilkent.edu.tr, hvdemir@ntu.edu.sg

^b School of Electrical and Electronic Engineering and School of Physical and Mathematical Sciences, Nanyang Technological University, 639798, Singapore.

^c Physical Chemistry, TU Dresden, Bergstrasse 66b, D-01062 Dresden, Germany.

† Electronic Supplementary Information (ESI) available: See

DOI: 10.1039/x0xx00000x

[†] These authors contributed equally to this paper.

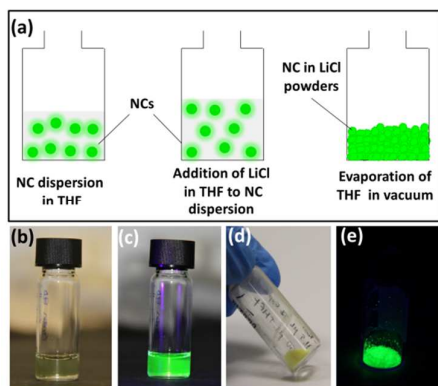


Figure 1. (a) Schematics of NC encapsulation into LiCl salt. The real colour images of NC dispersion in THF (b) under ambient lighting and (c) UV illumination at 366 nm. The real colour images of the NCs-in-LiCl powders (d) under ambient lighting and (e) UV illumination at 366 nm.

As a solution, here we propose and demonstrate incorporation of the nonpolar NCs directly into LiCl ionic salt without ligand exchange by benefiting from the solubility of LiCl in tetrahydrofuran (THF), which simultaneously disperses these nonpolar NCs. As a proof-of-concept demonstration, we integrated green-emitting CdSe/CdZnSeS/ZnS NCs into LiCl host (**Figure 1**) and characterized their structural and optical properties. In addition, we tested their emission stability on a blue LED operating at 100 mA for 96 h. At the end of the test, the NCs encapsulated in LiCl succeeded to preserve 95.5% of their initial emission intensity while that of the NCs without LiCl encapsulation decreased to 34.7%. To uncover the effect of the LiCl encapsulation on the emission capabilities of the NCs, we measured reproducibly the quantum efficiency of the NCs-in-LiCl host to be 75.1% which is higher than the quantum efficiency of the same as-synthesized nonpolar NCs in dispersion (73.1%) and the same ones in film without salt encapsulation (67.9%). Subsequently, we investigated the emission dynamics of the NCs-in-LiCl and observed that their radiative decay lifetime is consistent with the theoretical predictions relating the radiative lifetime to the variations of the dielectric environment. Considering all these, we believe that the proposed LiCl encapsulation of the nonpolar NCs will find wide-scale use in light-emitting devices as colour enrichment films of display backlights.

2. Results and discussion

We integrated nonpolar NCs-in-LiCl powders as described in the Experimental Methods section and **Figure 1**. Briefly, we mixed the oversaturated LiCl solution (in THF) with NCs dispersed in THF in a nitrogen environment. Subsequently, the solvent was evaporated under vacuum and consequently NC encapsulated powders were obtained. The NC weight percentage in these powders was determined to be $\sim 1.22\%$. Further structural characterizations were performed using scanning electron microscopy (SEM) and transmission electron microscopy (TEM) (**Figure 2**).

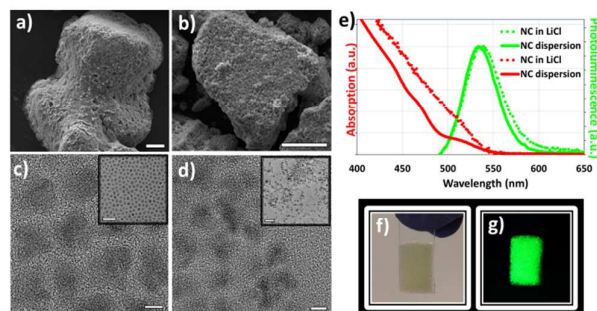


Figure 2. Scanning electron microscopy (SEM) images of the LiCl powders (a) without and (b) with NCs (scale bars: 30 μm). Transmission electron microscopy (TEM) images of (c) the as-synthesized NC dispersion in hexane and (d) the NC-in-LiCl powders (scale bars of larger images: 5 nm and inset images: 50 nm). (e) Photoluminescence spectra of the nonpolar NCs in dispersion and the same NCs encapsulated within LiCl ionic salt. Also, absorption spectra of the as-synthesized NCs (dispersion in hexane) and NC-in-LiCl powder film were provided. Real colour photographs of the LiCl encapsulated NC film under (f) ambient lighting and (g) UV illumination at 366 nm.

The SEM images of the representative LiCl powders with and without NC loading show that the size of the powders is in general less than 200 μm for both of the cases with and without NC loading and they do not exhibit crystal facets as opposed to slower crystallizations previously studied in other media¹³. This is mainly due to the fast evaporation of the solvent (THF in this case) under vacuum. Another interesting feature is the occurrence of small grape-like structures on the powders containing NCs while such an observation cannot be made for the LiCl powders without NC loading (**Figure S2(a),(b)**). Here it is worth noting that the NCs are small and cannot be imaged using SEM. Each of these grape-like structures most likely includes many NCs inside. We think that these grape-like structures may possibly take a role in preventing full aggregation of the NCs within LiCl and thus avoid the quenching of the NCs.

Furthermore, we used TEM to image the NCs without LiCl and the NCs incorporated in LiCl (**Figure 2(c)-(d)**). These images show that the size of our as-synthesized NCs is approximately 8 nm. In addition, we imaged the NC-in-LiCl powder (**Figures 2(d) and S3**) and observed that the NCs in LiCl tend to be localized in some parts of the salt. Finally, having the information of size and concentration of our NCs, we are able to estimate the molar concentration of the NCs inside LiCl host (see Electronic Supplementary Information (ESI) for the details). Our calculation reveals that there are between 13.0 and 18.4 pmol of NCs inside 1 mg of powder.

Following the morphological characterization, we prepared the NC-in-LiCl film as explained in the Experimental Methods section using a commercial epoxy that does not require any UV or heat treatment for hardening. Subsequently, we measured the steady-state photoluminescence spectra and quantum efficiencies of the NCs in the dispersion and encapsulated into LiCl host. We observed that the encapsulation of the NCs by the ionic salt causes a slight red shift in the emission spectrum (**Figure 2(e)**) as observed in previous works^{11,12}, which can be explained by the limited aggregation of the NCs within LiCl (**Figure 2(d)**, **Figure S3**) and also in part by the interactions of dipoles of the NCs with the dipoles of the surrounding medium

as also reported by Ibnaouf et al.¹⁵. The quantum efficiency of the NCs-in-LiCl was measured to be 75.1% while the quantum efficiency of the same NCs in dispersion was found to be 73.0% and that of the NCs without LiCl encapsulation in solid film remained at 67.9%. The observation of this increased quantum efficiency of the nonpolar NCs in the salt matrix agrees well with the previous reports of salt encapsulation of aqueous NCs in NaCl^{12,14}.

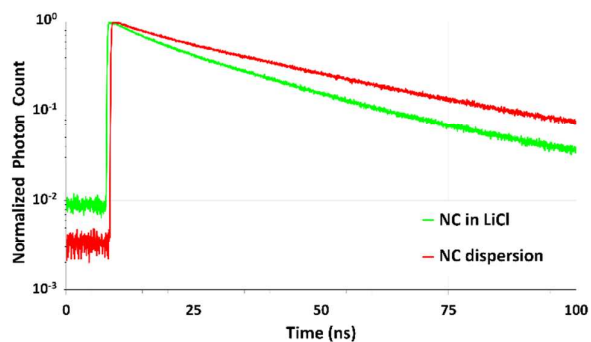


Figure 3. Time-resolved photoluminescence decay curves of the NCs in dispersion and the same NCs encapsulated in LiCl.

Here, we also analysed the emission kinetics of the NCs in dispersion and the same NCs encapsulated by the LiCl salt. The measured time-resolved photoluminescence spectra presented in **Figure 3** revealed a lifetime of 29.1 ns for the NCs dispersed in hexane and 19.4 ns for the NCs encapsulated in LiCl. Using the quantum efficiency (η) information together with the lifetime (τ_{total}), the effective radiative lifetime (τ_{rad}) is predicted using Equation 1.

$$\eta = \frac{1/\tau_{rad}}{1/\tau_{total}} \quad (1)$$

This analysis leads to a radiative lifetime of 39.9 ns for the NCs dispersed in hexane while that of the NCs-in-LiCl decreases to 25.8 ns. This decrease of the radiative decay time can be mainly attributed to the variation of the dielectric medium from the hexane in the case of the NC dispersion to LiCl in the case of the NC salt encapsulation. To test this hypothesis, we first calculated the radiative lifetime of the NCs in vacuum using the measured values in the dispersion by employing the virtual cavity, empty cavity, and fully-microscopic models¹⁶ (see ESI for details). Subsequently, we predicted the radiative lifetimes of the NCs using this value when they are surrounded by the LiCl matrix and present the results in Table 1 in the rows indicated by the names of these models. The computed results show that the predicted experimental and theoretical radiative lifetimes are reasonably close especially when the empty cavity model is considered. Therefore, we can conclude that the dipoles generated in the NCs encapsulated by the LiCl salt experience a radiative recombination that is not significantly affected by the local field of the surrounding medium generating the cavity.

In addition to the effect of the surrounding dielectric medium on the quantum efficiency, we also expect the ionic salts wrapping the NCs to improve the stability of the NC emission

on LEDs. For this purpose, we tested the emission stability of the NC-in-LiCl powders blended with epoxy on a blue LED driven at a high current level (**Figure 4(a)-(b)**) while the NCs without LiCl encapsulation blended with epoxy was our control group. We observed that the efficiency of the NCs without LiCl encapsulation decreased to 34.7% of its initial value after 96 h (four days) of uninterrupted operation while the film of NC-in-LiCl powders successfully preserved 95.5% of its initial quantum efficiency during the same period. In terms of the absolute quantum efficiencies, the quantum efficiency of the NC-in-LiCl powders decreased from 75.1% to 71.7% while that of the NCs without LiCl encapsulation dropped from 67.9% to below 23.6% at the end of the test (**Figure 4c**). We attribute this improvement in the emission stability of the NCs on a LED driven at high currents to the formation of a physical barrier against oxygen penetration by LiCl salt limiting the interaction with the ambient environment. This improved stability is of significant importance especially for the display backlighting.

Table 1. The quantum efficiency of the NCs in dispersion and the same NCs encapsulated in LiCl; their total lifetimes and radiative recombination lifetimes. In addition, the radiative lifetimes of the NCs in vacuum were first calculated by employing the radiative lifetime of the NCs in dispersion, then these values were used to predict the radiative lifetime of the NCs in LiCl matrix according to the empty cavity, virtual cavity, and fully microscopic models.

	Quantum Efficiency (%)	τ_{total} (ns)	τ_{rad} (ns)
NCs in dispersion	73.0	29.1	39.9
NCs-in-LiCl	75.1	19.4	25.8
Empty cavity model	-	-	28.7
Virtual cavity model	-	-	21.9
Fully microscopic model	-	-	32.5

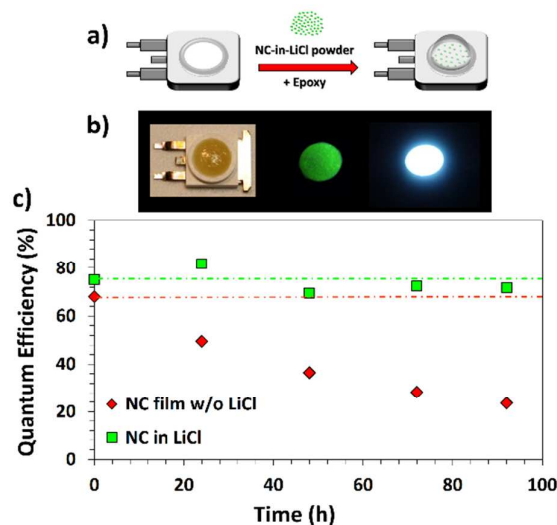


Figure 4. (a) Schematic image of NC-in-LiCl film preparation onto LED for temperature stability test. (b) Real colour images of the NCs-in-LiCl on a blue LED under ambient lighting, UV illumination at 366 nm, and when LED is driven, from left to right. (c) Quantum efficiency variation of the NCs with and without LiCl encapsulation as a function of time when they are integrated on the blue LED driven at a high current level for 96 h (four days).

To test whether a chemical interaction occurs between the ligands of the NCs and the host medium during crystallization

process, we measured the FTIR spectrum of the NCs without LiCl encapsulation, the NCs-in-LiCl, and the only LiCl salt (Figure S4). However, we could not see any indication of a potential chemical interaction. In order to gain further structural information, we performed thermal gravimetric analysis (TGA) on the samples of only NC, only LiCl, NC-in-LiCl powder and NC drop-casted LiCl powder (Figure S5, and see ESI for further details). We observe rapid evaporation of LiCl beyond its melting point (~605°C), and addition of NCs shifted this process toward lower temperatures. However, the characteristics of the weight loss curves of the NC-in-LiCl powders and NC drop-casted LiCl powders are very similar to each other, which tells us that this fastened evaporation is more likely a physical process rather than an indication of a chemical interaction. In addition, from the TGA curves we could not observe any signature that we can relate to any indication of the NCs-salt chemical interaction. As a result, using TGA, we were not able to identify an obvious chemical interaction between the NCs and the host matrix. To further investigate the interaction of the LiCl with the NCs, we performed X-ray photoelectron spectroscopy (XPS) of only NCs, NC-in-LiCl powders, and only LiCl powders (see ESI for further details, Figures S6 and S7). This analysis also did not provide any indication of a notable chemical interaction between the salt medium and the NCs.

3. Experimental

3.1 Chemicals: Cadmium oxide (CdO, 99.99 %), zinc acetate (Zn(acetate)₂, 99.9 %), sulfur (S, 99.9%), selenium (Se, 99.99%), potassium bromide (KBr) and lithium chloride (LiCl) were purchased from Sigma-Aldrich in powder form. Oleic acid (OA, 90 %), trioctylphosphine (TOP, 90 %), 1-octadecene (1-ODE, 90 %), dodecanethiol (DDT, 99 %), tetrahydrofuran (THF) and hexane were bought from Sigma-Aldrich and used without any purification.

3.2 NC synthesis: CdSe/CdZnSeS/ZnS nanocrystals were synthesized following the method in the literature¹⁷. For a typical synthesis, 0.4 mmol of CdO, 4 mmol of Zn(acetate)₂, 5.6 mL of OA and 20 mL of 1-ODE were loaded into a 50 mL three-neck flask. After degassing for 2 h at 100 °C under vigorous stirring, the temperature of mixture was raised to 310 °C under argon flow. At this temperature, 0.1 mmol of Se powder and 4 mmol of S powder both dissolved in 3 mL of TOP were quickly injected into the reaction flask. After 1 min, 0.3 mL of DDT dissolved in 0.8 mL of 1-ODE was injected dropwise and the temperature of the reaction flask was set to 300 °C. Following 10 min of growth, the mixture was cooled down to room temperature and precipitated with hexane/acetone mixture. Finally, the resulting nanocrystals were dissolved in hexane and used for further experiments.

3.3 Preparation of the LiCl encapsulated NC powders: Oversaturated stock solution of LiCl was prepared by mixing 1.83 g of LiCl in 50 mL of THF in a glovebox with nitrogen

environment. Prior to the encapsulation of the NCs-in-LiCl, hexane of the NC dispersion was evaporated. We optimized the NC amount to maximize their photoluminescence quantum efficiency in the salt (see Figure S1) and chose the sample with 0.4 mg of the NCs to use, which resulted in the highest quantum efficiency of 75.1%, throughout the rest of this work. Before the preparation of NC-in-LiCl powders, the NCs were first dispersed in 250 µL of THF, and then 1 mL of LiCl stock solution was slowly added on NCs in THF. Subsequently, the samples were placed within a desiccator to completely evaporate the solvent and to obtain the LiCl encapsulated NCs. NC weight percentage in the powders were determined by re-dissolving them in THF and comparing the NC absorbance values with the NC dispersion. The methodology for estimating molar concentration of the NCs inside the powders was explained in the ESI. Only LiCl powders were obtained using the same procedure without NC addition. The NC-in-LiCl films were prepared by mixing ~6.3 mg of the NC embedded LiCl powders with a commercial two-component epoxy (Bison), which does not require any UV or heat treatment for hardening. Since we aimed to test the stabilities of NC-in-LiCl powders on LEDs at a high current level, we chose this encapsulant on purpose. However, other encapsulants such as commercial silicones or poly(methyl methacrylate), which in general require heat treatment or UV exposure for hardening, can also be used with these powders.

3.4 Structural characterizations: Detailed information on SEM, TEM, FTIR, TGA, and XPS were provided in the ESI.

3.5 Steady-state and time-resolved fluorescence spectroscopy: Steady-state photoluminescence spectra of NC dispersion and NC-in-LiCl film were taken using a Spectral Products monochromator integrated Xenon lamp as the excitation source, a Hamamatsu integrating sphere, and an Ocean Optics Maya 2000 spectrometer. Time-resolved fluorescence spectra were taken using a PicoHarp 200 time-resolved single photon counting system (PicoQuant). A pulsed laser emitting at 375 nm was employed as the excitation source and the time difference between the time of the maximum photon count and the time of 1/e of maximum photon count was reported as the lifetime.

3.6 Quantum efficiency measurements: The quantum efficiency measurements were carried out at an excitation wavelength of 460 nm using a Spectral Products monochromator integrated Xenon lamp, a Hamamatsu integrating sphere, and an Ocean Optics Maya 2000 spectrometer using the following method, also previously described by deMello et al.¹⁸ This technique involves three steps: (i) the measurement of the spectrum when no sample is placed in the integrating sphere, (ii) the measurement of the spectrum when the sample is directly illuminated by the excitation source, and (iii) the measurement of the sample when the sample is not directly illuminated by the light source

and instead illuminated by the light scattered from the surface of the integrating sphere. Here, in step (ii), the sample was placed with a slight oblique angle as suggested. In step (iii), the sample was rotated so that only the scattered light excites the sample. In **Figure 5**, an illustration of this technique is presented and the quantum efficiency (η) is calculated using Equation 2. In this equation, E stands for the excitation part of the spectrum while L stands for the emission part of the measured spectrum. The subscripts i, ii, and iii indicate the measurement steps described above.

$$\eta = \frac{L_{ii} - E_{ii}L_{iii}/E_{iii}}{\left(1 - E_{ii}/E_{iii}\right)E_i} \quad (2)$$

The accuracy of the measurement setup was tested using Rhodamine 6G dissolved in ethanol with an optical density <0.1 at 460 nm. We measured a quantum efficiency of 94.7%, which is in agreement with the standard value of 95%.

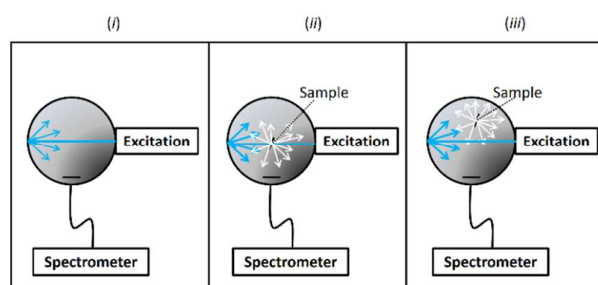


Figure 5. Illustration of the quantum efficiency measurement methodology: (i) The measurement of the excitation spectrum without sample, (ii) the measurement of the spectrum when the sample is directly excited by the light source, and (iii) the measurement of the spectrum when the sample is excited by the light that scatters from the surface of the integrating sphere.

3.7 Emission stability tests: The emission stability of the films were tested by investigating the emission intensity of the NCs with and without LiCl encapsulation on an Avago ASMT blue LED driven at 100 mA for 96 h (four days). The NCs with LiCl encapsulation were coated on the LED chip using the two-component epoxy. As the control group, the NCs without LiCl were coated on the blue LED by first drop-casting the NCs on the LED and then the epoxy was added and blended with the NCs following the evaporation of the solvent.

4. Conclusions

In summary, here we present the encapsulation of the colloidal as-synthesized nanocrystals by the LiCl ionic salts in the form of powder, which significantly improves the stability of the encapsulated NCs on LEDs operating at high currents. We also observed that the LiCl encapsulation helps preserving the dispersion quantum efficiency levels of the NCs for use in the colour enrichment films. Additionally, unlike the previous reports on the incorporation of the aqueous NCs in salt or sucrose matrices, this

method totally removes the need for a ligand exchange of the nonpolar NCs, which is known to otherwise suffer from decreased quantum efficiencies during the phase transfer. Considering all these strong aspects, we believe that the proposed encapsulation technique presented here will find a wide-spread use in the light-emitting diodes of display backlights integrated with NCs as colour enrichment films.

Acknowledgements

We acknowledge ESF EURYL, EU-FP7 Nanophotonics4Energy NoE, BMBF TUR 09/001, and TUBITAK EEEAG 109E002, 109E004, 110E010, 110E217, 112E183 and in part by NRF-CRP-6-2010-02 and NRF-RF-2009-09. H.V.D. acknowledges additional support from TUBA-GEBIP and T.E. acknowledges support from TUBITAK BIDEB.

Notes and references

‡ Electronic Supplementary Information (ESI) available: See DOI: 10.1039/x0xx00000x

§ Talha Erdem and Zeliha Soran-Erdem contributed equally to this work.

- R. Rossetti, J. Ellison, J. Gibson, L. Brus, *J. Chem. Phys.*, 1984, **80**, 4464-4469.
- Nat. Nanotech.*, 2014, **9**, 325.
- X. Michalet, F. F. Pinaud, L. A. Bentolila, J. M. Tsay, S. Doose, J. J. Li, G. Sundaresan, A. M. Wu, S. S. Gambhir, S. Weiss, *Science*, 2005, **307**, 538-544.
- T. Erdem, H. V. Demir, *Nanophoton.* 2013, **2**, 57-81.
- H. V. Demir, S. Nizamoglu, T. Erdem, E. Mutlugun, N. Gaponik, A. Eychmüller, *Nano Today*, 2011, **6**, 632-647.
- X. Yang, Y. Ma, E. Mutlugun, Y. Zhao, K. S. Leck, S. T. Tan, H. V. Demir, Q. Zhang, H. Du, X. W. Sun, *ACS Appl. Mater. Interfaces*, 2014, **6**, 495-499.
- C. Dang, J. Lee, C. Breen, J. S. Steckel, S. Coe-Sullivan, A. Nurmikko, *Nat. Nanotech.*, 2012, **7**, 335-339.
- B. Guzelturk, Y. Kelestemur, M. Z. Akgul, V. K. Sharma, H. V. Demir, *J. Phys. Chem. Lett.*, 2014, **5**, 2214-2218.
- E. Jang, S. Jun, H. Jang, J. Lim, B. Kim, Y. Kim, *Adv. Mat.*, 2010, **22**, 3076-3080.
- S. Jun, J. Lee, E. Jang, *ACS Nano*, 2013, **7**, 1472-1477.
- T. Otto, M. Müller, P. Mundra, V. Lesnyak, H. V. Demir, N. Gaponik, A. Eychmüller, *Nano Lett.*, 2012, **12**, 5348-5354.
- M. Müller, M. Kaiser, G. M. Stachowski, U. Resch-Genger, N. Gaponik, A. Eychmüller, *Chem. Mater.*, 2014, **26**, 3231-3237.
- T. Erdem, Z. Soran-Erdem, P. L. Hernandez-Martinez, V. K. Sharma, H. Akcali, I. Akcali, N. Gaponik, A. Eychmüller, H. V. Demir, *Nano Res.*, 2015, **8**, 860-869.
- Z. Soran-Erdem, T. Erdem, P. L. Hernandez-Martinez, M. Z. Akgul, N. Gaponik, H. V. Demir, *J. Phys. Chem. Lett.*, 2015, **6**, 1767-1772.
- K. H. Ibnaouf, S. Prasad, M. S. Al Salhi, A. Hamdan, M. B. Zaman, L. El Emir, *J. Lumin.*, 2014, **149**, 369-373.
- S. F. Wuister, C. de Mello Donega, A. Meijerink, *J. Chem. Phys.*, 2004, **121**, 4310-4315.
- W. K. Bae, K. Char, H. Hur, S. Lee, *Chem. Mater.*, 2008, **20**, 531-539.
- J. C. de Mello, H. F. Wittmann, R. H. Friend, *Adv. Mater.*, 1997, **9**, 230-232.